

Fitting the Galactic Center Gamma-Ray Excess with Cascade Annihilations

Adam Martin,¹ Jessie Shelton,² and James Unwin¹

¹*Department of Physics, University of Notre Dame, Notre Dame, IN, 46556, USA*

²*Department of Physics, University of Illinois, 1110 West Green Street, Urbana, IL 61801, USA*

The apparent excess of gamma rays in an extended region in the direction of the galactic center has a spatial distribution and amplitude that are suggestive of dark matter annihilations. If this excess is indeed due to dark matter annihilations, it would indicate the presence of both dark matter and an additional particle beyond the Standard Model that mediates the interactions between the dark matter and Standard Model states. We introduce reference models describing dark matter annihilation to pairs of these new mediators, which decouples the SM-mediator coupling from the thermal annihilation cross section and easily explains the lack of direct detection signals. We determine the parameter regions that give good descriptions of the gamma ray excess for several motivated choices of mediator couplings to the SM. We find fermion dark matter with mass 7-26 GeV and a dark vector mediator, or scalar dark matter in the 10-50 GeV range (Higgs portal mediator) or 10-65 GeV range (gluophilic mediator) can provide a comparable or improved fit, compared to the case of direct annihilation. We demonstrate that these models can easily satisfy all constraints from collider experiments, direct detection, and cosmology.

I. INTRODUCTION

The existence of some form of dark matter (DM) is well-established from its gravitational interactions. The coincidence that the Standard Model (SM) weak interactions roughly coincide with the coupling strength required for the thermal freeze-out of a weak scale particle to account for the observed relic abundance has driven a multipronged search for non-gravitational signals of DM, in direct detection experiments, in cosmic ray signals, and at colliders. Over the last few years an excess of gamma rays over astrophysical predictions has been observed in the Fermi-LAT data in the direction of the galactic center (GC) [1–10]. The extended and spherically symmetric spatial distribution, the overall rate, and the shape of the spectrum associated with the excess are strikingly consistent with an origin in annihilating DM. Of course, astrophysical sources of the excess are still a possibility. Millisecond pulsars have been proposed as a source for the excess [11, 12]; however, such a population would have to be novel in both its spatial and luminosity distributions [6, 8, 10, 13]. In particular, the fact that the excess appears to extend well beyond the GC, out to at least around 10° , is a challenge for the millisecond pulsar interpretation. It has also been suggested that the excess could be due to cosmic ray interactions with gas and dust [1, 3, 4, 7], but similarly it has been argued that these explanations provide a poor fit to the data [14, 15].

One of the most intriguing features of the GC gamma ray excess is that if it is indeed due to DM, then it would establish the existence not only of DM but also of some new mediator particle responsible for its interaction with the SM. The spectrum of the excess has been fit well by DM annihilations $X\bar{X} \rightarrow b\bar{b}$, in which case the DM mass is $m_{\text{DM}} \approx 30$ GeV; annihilations $X\bar{X} \rightarrow \tau\bar{\tau}$ provide a less good fit to the data and would point to lighter masses. Intriguingly, with these hypotheses for the annihilation, the cross-section needed to achieve the rate seen in the excess is strikingly close to the thermal value:

$\sigma v \sim 10^{-26}$ cm³/s [10]. However, this mass range for DM, $20 \text{ GeV} \lesssim m_{\text{DM}} \lesssim 40 \text{ GeV}$, has been very well studied by direct detection experiments. The two SM particles capable of mediating $X\bar{X} \rightarrow f\bar{f}$ are the Higgs and the Z boson. With the coupling to DM set by the deduced cross-section $X\bar{X} \rightarrow f\bar{f}$, both the Higgs and the Z would give rise to direct detection signals vastly in excess of observations. In addition, the failure to observe $h \rightarrow X\bar{X}$ at the LHC independently eliminates the 125 GeV Higgs as a mediator for the DM annihilations. Thus some beyond-the-SM field is required to mediate DM annihilations to the SM, whether heavy [16, 17] or light [18–21]. Other implications and aspects of model building have been considered in e.g. [22–31].

In the present work we highlight the possibility that the mediator may easily be lighter than the DM, in which case DM will typically annihilate to pairs of on-shell mediators rather than directly to SM particles. In this case, constraints from LHC and direct detection experiments can be almost entirely obviated [32]. Thermal freeze-out determines the coupling of DM to the mediators, but the coupling of the mediators ϕ to the SM is a free parameter. Whilst the coupling of ϕ to the SM is constrained by collider and direct detection searches on one hand, and by the requirement that they decay before Big Bang nucleosynthesis (BBN) on the other, a wide range of values are still permitted by all available data. This allows direct detection signals to be small while still maintaining a thermal annihilation rate. We construct three simple reference models, coupling the mediators to the SM through the hypercharge portal, through the Higgs portal, and through the gluonic operators $G_{\mu\nu}^a G^{a\mu\nu}$ and $G_{\mu\nu}^a \tilde{G}^{a\mu\nu}$, and establish the region of cascade annihilation parameter space that yields a good explanation for the GC excess.

The paper is structured as follows: In Sect. II we examine the photon spectra coming from DM cascade annihilations to SM states and identify the best-fit parameter regions which reproduce the spectrum of the inner galaxy

gamma ray excess. In Sect. III - V, we present simple reference models which yield cascade annihilations capable of describing the excess, and discuss the viable parameter space. We examine the relevant limits and discuss the prospect for signals at colliders and direct detection experiments. Finally in Sec. VI we conclude.

II. FITTING THE EXCESS WITH DARK MATTER CASCADE ANNIHILATIONS

In this section we examine the photon spectra that result from DM cascade annihilations

$$X\bar{X} \rightarrow \phi\phi \rightarrow f\bar{f}f'\bar{f}', \quad (1)$$

as illustrated in Fig. 1. We study how the spectra vary with respect to m_{DM} and m_{med} , and determine which combinations of new particle masses and SM final states provide a good fit to the shape of the spectrum extracted in [10].

The flux of gamma rays $\Phi(E_\gamma, \psi)$ produced at energy E_γ due to annihilating DM with mass m_{DM} , as a function of angle of observation ψ , is given by

$$\frac{d^2\Phi}{d\Omega dE_\gamma} = \frac{\langle\sigma v\rangle}{8\pi\eta m_{\text{DM}}^2} \left(\sum_f \frac{dN}{dE_\gamma} \text{Br}_f \right) J(\psi, \gamma), \quad (2)$$

where $\langle\sigma v\rangle$ is the thermally averaged DM annihilation cross section, Br_f is the branching ratio to a given final state f , and the sum runs over all final states. The flux also depends on whether the DM is complex ($\eta = 2$) or self-conjugate ($\eta = 1$). Unless stated otherwise, we shall assume that the DM is non-self-conjugate (e.g. Dirac) and accordingly take $\eta = 2$. The factor J is the line-of-sight integral (see e.g. [33])

$$J(\psi, \gamma) = \int_{\text{LOS}} \rho^2(r) dl, \quad (3)$$

which depends on the distribution of the DM $\rho(r)$ as a function of radial distance from the GC. Previous studies

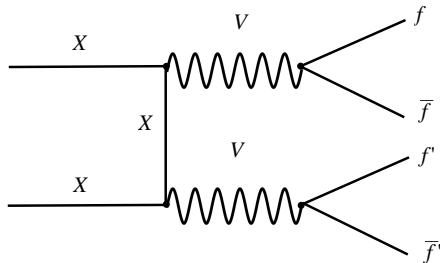


FIG. 1. Dark matter (particle X) cascade annihilation diagram to Standard Model fermion pairs $f\bar{f}$ via intermediate states V .

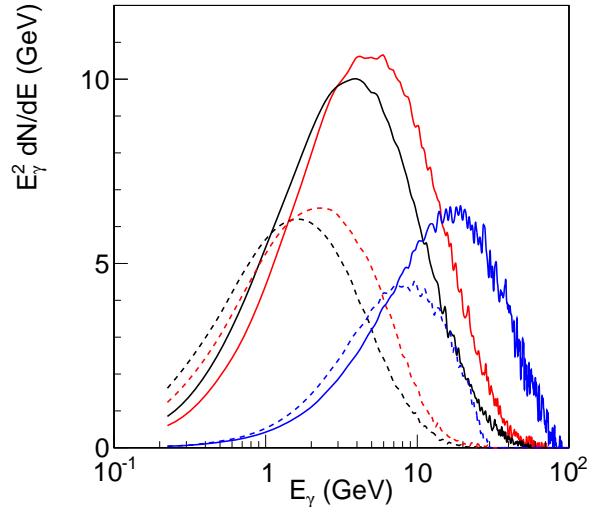


FIG. 2. Examples of photon spectra (from Pythia 8) assuming DM annihilation to $c\bar{c}$ (red), $b\bar{b}$ (black), $\tau\bar{\tau}$ (blue). For direct decays with $m_{\text{DM}} = 30$ GeV (dotted) and cascade decays with $m_{\text{DM}} = 100$ GeV and $m_V = 30$ GeV (solid).

[1–10] have established that the spatial distribution of the gamma ray excess is well-fit by a generalised Navarro-Frenk-White (NFW) distribution [34, 35]

$$\rho(r) = \rho_0 \frac{(r/r_s)^{-\gamma}}{(1 + r/r_s)^{3-\gamma}}, \quad (4)$$

with best-fit shape parameter $\gamma \simeq 1.26$ [10], local DM density $\rho_0 = 0.3$ GeV/cm³, and scale radius r_s which we take to be 20 kpc. These values are in agreement with the suggested range in [36]. The normalization of the gamma ray signal depends on the product $J\langle\sigma v\rangle$. It is important to note that uncertainties in the astrophysical distribution of DM complicate the determination of the thermal cross-section. We will adopt the absolute normalization of the excess as determined in [10] together with their best-fit $\rho(r)$, and report on the deduced cross-section $\langle\sigma v(X\bar{X} \rightarrow \phi\phi)\rangle$ needed to fit the rate. We compare this to predictions from specific thermal reference models in Sects. III - V.

Our first step is to establish which combinations of masses and final states yield a good description of the shape of the photon spectrum. For a given DM mass and final state we determine the photon spectra using Pythia 8 [37]. Example spectra for DM annihilations to either b, c or τ final states are plotted below in Fig. 2. We show examples of both direct annihilations $X\bar{X} \rightarrow f\bar{f}$ and cascade annihilations $X\bar{X} \rightarrow f\bar{f}f'\bar{f}'$. Shifting from direct to cascade annihilations affects both the height and peak location in the $E_\gamma^2 dN/dE$ distributions.

For a given choice of m_{DM} , m_{med} and final state, we fit the resulting photon spectrum to the data shown in [10]. To perform this fit, we fix the normalization of each $E_\gamma^2 dN/dE$ curve so that the integrated flux of the

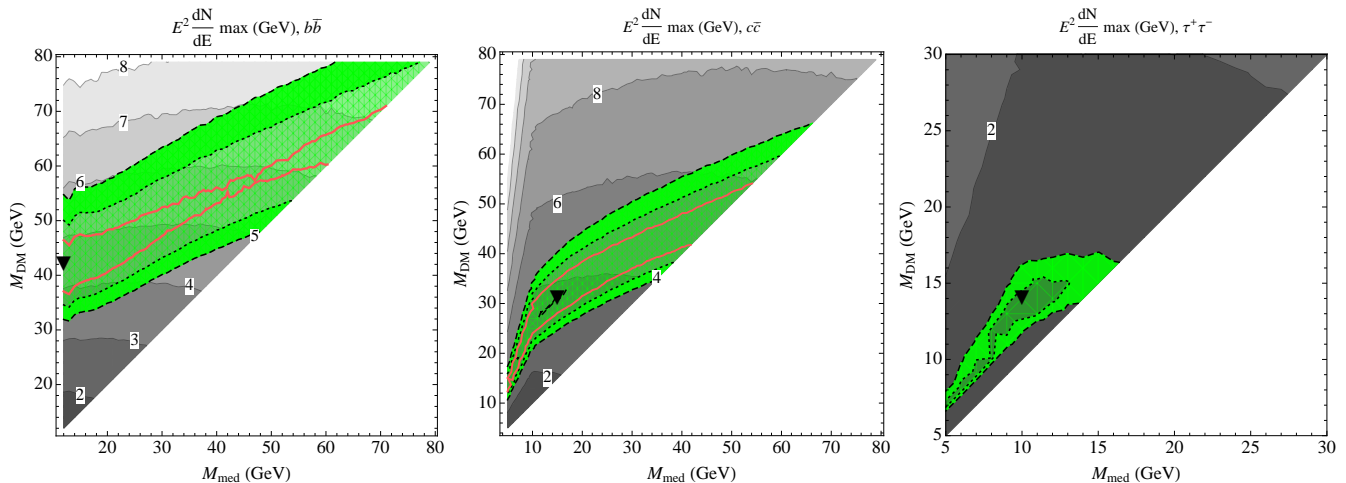


FIG. 3. Contour plots of $\max \left[E_\gamma^2 \frac{dN}{dE_\gamma} \right]$ as a function of m_{DM} and m_{med} for cascade decays to $b\bar{b}$, $c\bar{c}$, $\tau\bar{\tau}$ (grey contours). For a spectrum which fits the shape of the flux, the corresponding value of $\max \left[E_\gamma^2 \frac{dN}{dE_\gamma} \right]$ may be used to obtain the normalization factor $J\langle\sigma v\rangle$ required to match the signal. Parameter regions that provide a good fit to the observed spectrum are highlighted in green, showing contours of χ^2 . Parameter space within the red curves indicates a better fit than achieved for the case of direct annihilations, as identified in [10]. The black markers indicate the best fit points for each case. Further details are given in the text.

cascade model is normalised to the flux reported in [10]. We then define a χ -square statistic that compares the predicted flux from a given cascade model in each bin N_i^{mod} to the observed flux N_i^{data} , as given in [10], and sums over the bins

$$\chi^2 = \sum_i \frac{(N_i^{\text{data}} - N_i^{\text{mod}})^2}{\sigma_i^2}, \quad (5)$$

where σ_i is the error on the data. Contours of the best fit regions in the m_{DM} , m_{med} plane that give good fits to the shape of the photon spectrum for cascade annihilations to different final states are shown in Fig. 3. The green contours show the best fit region according to the χ^2 test¹; the inner contour corresponds to $\chi^2/\text{d.o.f} = 2$, and the outer contour is $\chi^2/\text{d.o.f} = 3$. The χ^2 contours are overlaid over grey contours of $\max \left[E_\gamma^2 \frac{dN}{dE_\gamma} \right]$, normalized to half the number of photons per annihilation. For spectra that fit the data well, the $\max \left[E_\gamma^2 \frac{dN}{dE_\gamma} \right]$ can then be used to determine the normalization factor $J\langle\sigma v\rangle$ necessary to fit the observed flux.

The red line in Fig. 3 corresponds to a fit of quality comparable to that found by [10] for direct annihilations; the best fit DM mass for $X\bar{X} \rightarrow b\bar{b}$ was identified as $m_{\text{DM}} \simeq 32.25$ GeV with $\chi^2/\text{d.o.f} = 1.4$.² Thus the parameter space which lies within the red curves provides an improved fit, which is not unexpected as the cascade

scenario introduces additional parameters. The lack of a red curve in the rightmost panel of Fig. 3 means all $(m_{\text{med}}, m_{\text{DM}})$ points lead to spectra with $\chi^2/\text{d.o.f} > 1.4$.

We consider only prompt photons, meaning photons from decay of or radiation off the final state. Secondary photons arising from the interaction of DM annihilation products with dust, gas, and magnetic fields (and, to a lesser extent, with starlight and the CMB) can be important for accurately extracting and understanding the spectrum of the DM annihilations [38]. The magnitude and morphology of these secondary contributions depend on the distribution of matter and radiation in the galaxy. Away from the galactic disk, we expect the contribution of secondary photons to be relatively unimportant, and, following [10] we fit to the flux as determined at $\psi = 5^\circ$ where bremsstrahlung and other secondary processes can largely be neglected.

In Fig. 4 we show the corresponding plots for cascade annihilations to mediators with specific choices of branching fractions to SM fermions. We consider three scenarios for the coupling of the mediator to the SM. First, we consider the case where the mediator is a vector boson V , coupling to the SM via the hypercharge portal, $\epsilon F_{\mu\nu} B^{\mu\nu}$ [39, 40]. For $m_V \lesssim 20$ GeV, the branching fractions of the V to SM fermions are approximately proportional to electric charge; for heavier m_V , the branching fractions begin to become more Z -like. We use the mass-dependent branching fractions, determined at tree level (see, e.g., [41]). Second, we consider the case where the mediator is a scalar, which couples to the SM via the Higgs portal, and has branching fractions given at tree-level by the SM Yukawa couplings. In our numerical work we use branching fractions computed by HDECAY [42, 43], includ-

¹ We give the ratio of χ^2 relative to the $(25 - 1)$ degrees of freedom, corresponding to the 25 data points used in the analysis of [10].

² To be consistent, this is the χ^2 calculated by our procedure for 32.25 GeV DM annihilating to $b\bar{b}$, not the value quoted by [10].

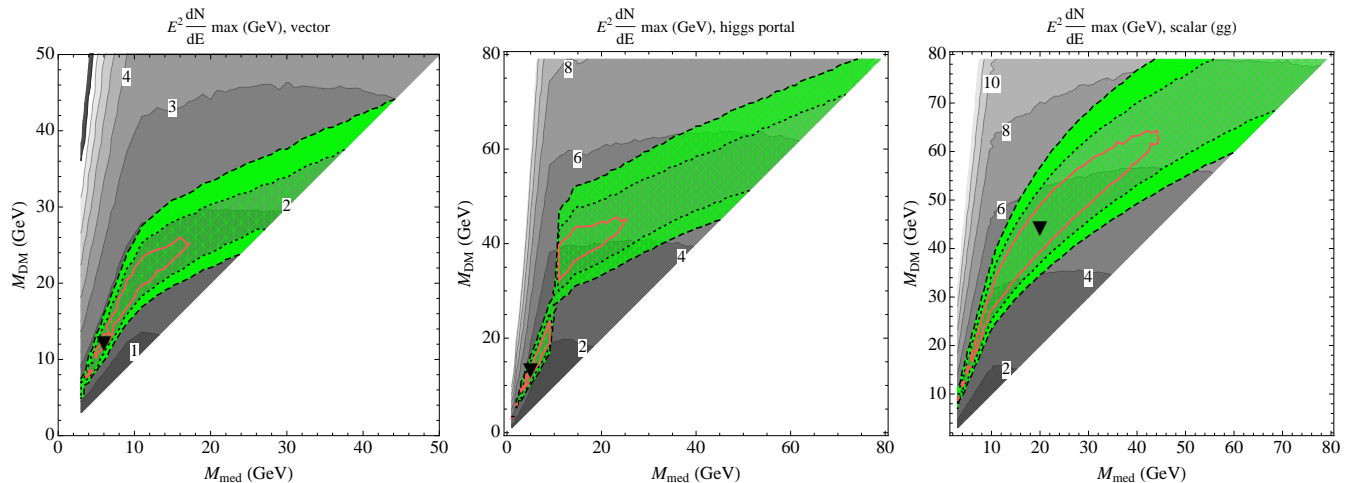


FIG. 4. As in Fig. 3, for specific choices of mediator. The left panel corresponds to a dark vector mediator $X\bar{X} \rightarrow V_\mu V^\mu$, with V^μ coupling to the SM through the hypercharge portal, as discussed in Sect. III. Cascade annihilation to scalar states $X\bar{X} \rightarrow ss$ which subsequently decay to SM fermions through the Higgs portal, Sect. IV, is shown in the center panel. The right panel shows annihilation $X\bar{X} \rightarrow aa$, with $a \rightarrow gg$, as discussed in Sect. V. The black markers indicate the best fit points.

ing higher-order corrections and the loop-induced mode $h \rightarrow gg$. Finally, we consider the case where the mediator is a (pseudo-)scalar coupling to the SM through the higher dimensional operators $a G_{\mu\nu}^a \tilde{G}^{a\mu\nu}$ or $s G_{\mu\nu}^a G^{a\mu\nu}$, resulting in $a(s) \rightarrow gg$. Further, in Fig. 5 we show the corresponding flux for the best fit of each of the cases studied in Fig. 4, using the preferred astrophysical parameters identified in [10].

One expected consequence of fitting the spectrum with cascade annihilations is the expanded range of m_{DM} that can yield a good description of the shape. Generically cascade annihilations point to heavier DM masses than do direct annihilations. The diagonal line where $m_{\text{DM}} = m_{\text{med}}$ recovers the spectra for direct annihilations, $X\bar{X} \rightarrow f\bar{f}$, at the mass

$$m_{\text{DM}}|_{\text{direct}} = 0.5 m_{\text{DM}}|_{\text{cascade}} , \quad (6)$$

with *twice* as many photons per event. This limit is not of particular interest for describing the observed GC photon excess, as the thermal cross-section is proportional to $\beta_f = \sqrt{1 - m_{\text{med}}^2/m_{\text{DM}}^2}$, and becomes velocity-suppressed in the degenerate limit. Cascade annihilations are a more compelling scenario away from the diagonal line. It is therefore interesting that in all cases our best-fit regions lie at $m_{\text{med}}/m_{\text{DM}} < 1$.

Given that the ratio of masses should be $m_{\text{med}}/m_{\text{DM}} \gtrsim 0.1$ in order to reproduce the shape of the 1-3 GeV photon excess, the dark mediator is not in a regime in which Sommerfeld effects are typically important, see e.g. [44]. The DM elastic self-interactions resulting from mediator exchange are thus not in the range that could account for the astrophysical small scale structure anomalies, such as the core-vs-cusp problem, for which self-interacting DM models substantially lighter mediators have been proposed as a solution [45, 46]. Conversely, the cascade an-

ihilation scenarios we consider here are not constrained by limits on DM-DM self-scattering, such as those arising from the observation of elliptical halos [47].

Another noticeable feature of the left and middle panels of Fig. 4 is the change in shape of the χ^2 contour around $m_{\text{med}} = 10$ GeV, where the $\rightarrow \bar{b}b$ final state becomes accessible.

III. CASCADE ANNIHILATION TO VECTOR MEDIATORS

In this section we construct an explicit reference model for DM annihilating to pairs of vector bosons, and discuss direct detection and LHC constraints. The regions of DM mass and vector mass that yield good fits to the GC excess are shown in Fig. 4.

We take the DM to be a Dirac fermion χ , interacting with a massive dark vector V_μ with coupling strength g_D , and couple the dark vector to the SM through the hypercharge portal, $\mathcal{L} = \epsilon B_{\mu\nu} V^{\mu\nu}$. This kinetic mixing couples V_μ to SM fermions, thereby destabilizing V_μ , and yielding a direct detection signal. The relic abundance of χ is set by its annihilation to pairs of vectors, $\chi\bar{\chi} \rightarrow VV$. This process has an *s*-wave contribution, and thus yields present-day annihilation cross-sections of the correct order of magnitude to explain the GC excess. Both the direct detection cross-section and the V_μ total width are proportional to ϵ^2 . On one hand, V_μ must decay sufficiently promptly to avoid disrupting the predictions of BBN. On the other hand, the direct detection cross-section must be small enough not to conflict with LUX bounds [48]. Thus, the admissible range of mediator-SM couplings is bounded [49].

In what follows, we fix the dark coupling constant g_D to

the value that yields the correct thermal relic abundance for χ . The thermal annihilation cross-section is

$$\langle\sigma v\rangle = \frac{\pi\alpha_D^2(1 - m_V^2/m_\chi^2)^{3/2}}{m_\chi^2(1 - m_V^2/2m_\chi^2)^2} + \mathcal{O}(v^2). \quad (7)$$

Requiring $\Omega h^2 = 0.112$ fixes $\alpha_D \equiv g_D^2/4\pi$ for given m_V, m_χ . Note we are working in the limit where the Born approximation holds, i.e. where $\alpha_D m_\chi/m_V < 1$, and enhancements to cross-sections at low velocities are negligible. The resulting value for α_D is shown in Fig. 6 (left), where we have used the standard analytic approximate solution to the Boltzmann equation assuming s -wave freeze-out. This is a good approximation for $x \equiv m_V/m_\chi \lesssim 0.7$ and a not unreasonable approximation for $0.7 \lesssim x \lesssim 0.9$. In the degenerate limit $m_V \rightarrow m_\chi$, the s -wave term in the v^2 expansion vanishes, and the resulting thermal annihilation cross-section is highly velocity-suppressed; we consider this region of parameter space of less interest for explaining the excess in the GC.

For the best-fit region of m_V, m_χ indicated in Fig. 4, exactly solving the Boltzmann equation predicts that the

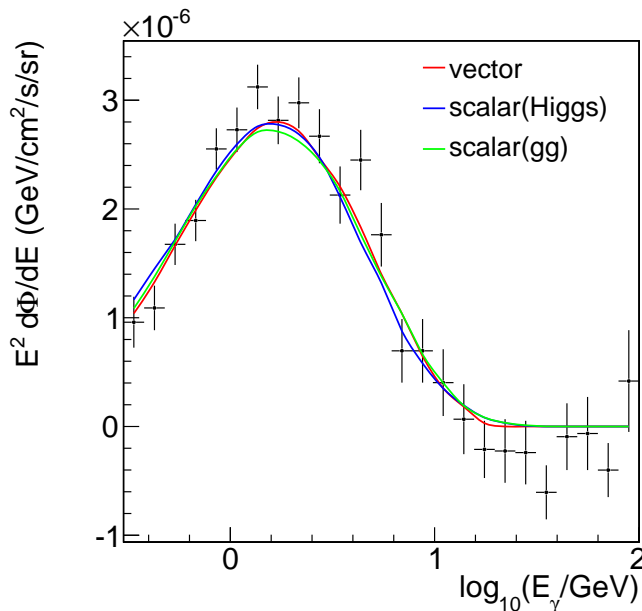


FIG. 5. Gamma-ray flux observed in the inner galaxy, as reported by [10], compared to the best-fit spectra for each model of DM cascade annihilation. Red: Dark vector model with $m_{\text{DM}} = 22$ GeV and $m_{\text{med}} = 12$ GeV, for DM annihilation cross section of $\langle\sigma v\rangle = 3.4 \times 10^{-26}$ cm³/s. Blue: Scalar decaying via the Higgs portal for $m_{\text{DM}} = 40$ GeV and $m_{\text{med}} = 20$ GeV, for $\langle\sigma v\rangle = 4.4 \times 10^{-26}$ cm³/s. Green: Scalar decaying to gluons with $m_{\text{DM}} = 60$ GeV and $m_{\text{med}} = 40$ GeV, for $\langle\sigma v\rangle = 6.1 \times 10^{-26}$ cm³/s. In each case the flux is calculated for angular direction 5° from GC, for a generalised NFW profile with $\gamma = 1.26$ and $\rho_0 = 0.3$ GeV/cm³.

thermal cross-section today lies in the range

$$\langle\sigma v\rangle|_{\text{today}} = (4.3 - 4.5) \times 10^{-26} \text{ cm}^3/\text{s}. \quad (8)$$

Fixing the dark coupling constant to yield the thermal relic abundance, direct detection experiments then constrain the coupling of the dark vector to the SM. The direct detection cross-section per nucleon is

$$\sigma_{\chi n} = \frac{g_D^2 \bar{g}_N^2}{\pi m_\chi^4} \mu^2, \quad (9)$$

where μ is the DM-nucleon reduced mass, and \bar{g}_N is the average nuclear coupling,

$$\bar{g}_N^2 \equiv \left(\frac{Zg_p + (A - Z)g_n}{A} \right)^2. \quad (10)$$

In Eq. (9), we have kept the leading contribution from V_D exchange only, neglecting the subleading contributions from Z exchange, which are suppressed by $\mathcal{O}(m_V^2/m_Z^2)$. This is a good approximation in the best-fit regions for the vector model.

In the right panel of Fig. 6, we plot the maximum allowed ϵ as a function of DM and vector masses. To generate this plot we have used the approximate analytic s -wave relic abundance calculation to determine the thermal value of α_D . For a given coupling α_D appropriate to obtain the observed DM relic density, as determined in Fig. 6 (left), one can satisfy the LUX bound by taking ϵ smaller than the (upper bound) contours of Fig. 6 (right). The values of ϵ required to satisfy LUX limits still allow the dark vector to decay long before BBN.

The cosmological history of the dark sector also depends on ϵ weakly through the temperature T_{dec} when χ and the SM depart from kinetic equilibrium. The kinetic mixing sets the strength of interactions of the form $\chi f \rightarrow \chi f$, and for $\epsilon \ll 1$, DM-SM scattering may drop below the Hubble expansion. Once this kinetic decoupling occurs, SM species leaving the thermal plasma deposit their entropy only into lighter SM particles, and the SM is accordingly hotter than the dark matter. Setting $n_f \sigma v(\chi f \rightarrow \chi f) \lesssim H(T)$, we estimate

$$T_{\text{dec}}^2 \approx (10 \text{ MeV})^2 \left(\frac{0.003}{\alpha_D} \right) \left(\frac{m_V}{10 \text{ GeV}} \right)^4 \times \left(\frac{20 \text{ GeV}}{m_\chi} \right) \left(\frac{10^{-4}}{\epsilon} \right)^2 \left(\frac{4}{\sum g_i Q_i^2} \right), \quad (11)$$

where the sum runs over the relativistic visible sector states carrying charge Q , with internal degrees of freedom g_i , but for the case at hand this is simply the electron. Thus χ stays in kinetic equilibrium with the SM well below the freeze-out temperature in our best-fit region, provided ϵ is not too far below current bounds. Accordingly, in our calculation above we have for definiteness taken $T_{\text{DM}} = T_{\text{SM}} = T$. For $\epsilon \lesssim 10^{-6}$, a complete treatment of kinetic decoupling would be required for a precise prediction of the present-day annihilation cross-section.

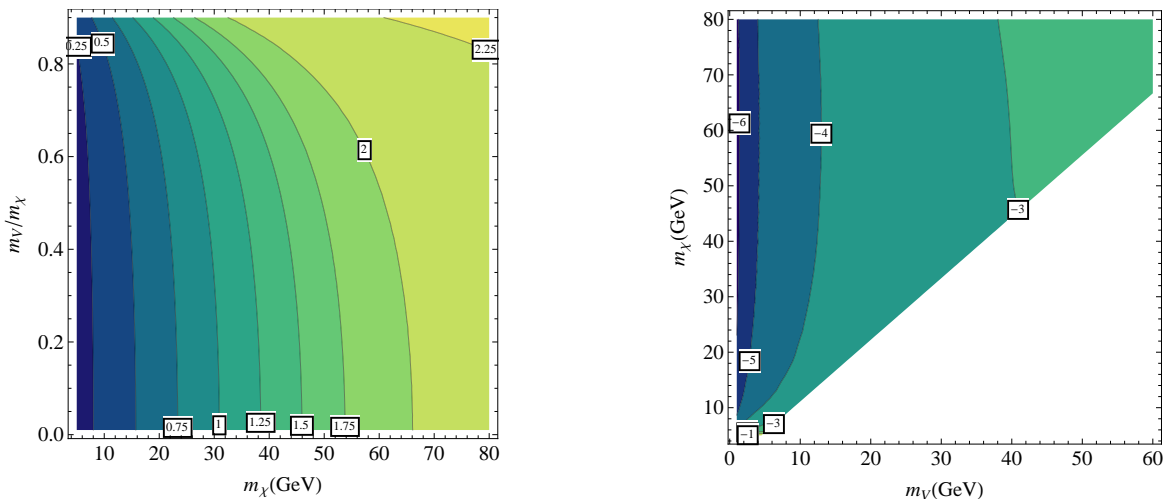


FIG. 6. Left: The dark gauge coupling required to obtain $\Omega h^2 = 0.11$ for Dirac fermion DM χ annihilating to pairs of dark gauge bosons V , as a function of m_χ and $m_V = xm_\chi$ (using the approximated s -wave solution to the Boltzmann equation). Contours show the required value of α_D in units of 10^{-3} . Right: The maximum value of the kinetic mixing parameter ϵ allowed by LUX [48], when the dark coupling constant α_D has been set to its thermal relic value. Contours of $\log_{10} \epsilon$ are shown.

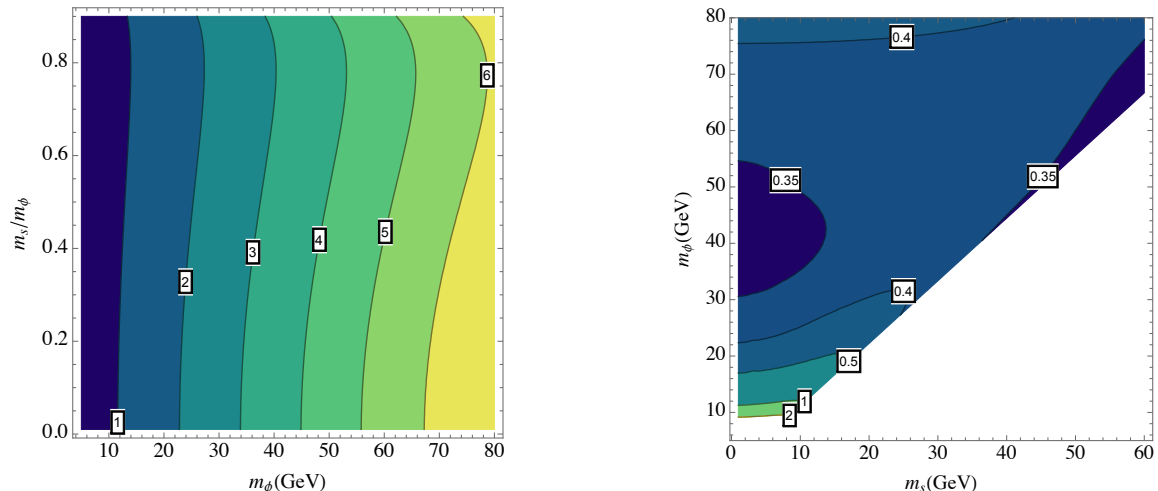


FIG. 7. Left: The quartic coupling λ_4 needed to obtain $\Omega h^2 = 0.11$ for complex scalar DM ϕ annihilating to pairs of dark scalars s in the reference model of Eq. (12), as a function of m_ϕ and $m_s = xm_\phi$ (using the approximated s -wave solution to the Boltzmann equation). Contours show the required value of λ_4 in units of 10^{-2} . Right: The approximated maximum value of the Higgs mixing parameter ϵ allowed by LUX [48], when the dark quartic coupling λ_4 has been set to its thermal relic value. In both panels we have set $y = 1$.

So long as kinetic decoupling occurs prior to the chiral phase transition, these corrections are small in comparison to the current astrophysical uncertainties.

There are many experimental constraints on kinetically mixed $U(1)$ s; see [50] for a summary. For dark vector masses $m_V > 10$ GeV, the most stringent constraints come from electroweak precision measurements, and limit $\epsilon \lesssim 0.02$ for most values of m_V below the Z pole [51]. For dark vectors lighter than $m_\gamma \approx 9.5$ GeV there are more stringent limits from invisible quarkonium decay [52], constraining the mediator couplings to be $\epsilon \lesssim 10^{-3}$.

These bounds do not significantly constrain the region of parameter space that is allowed by LUX.

This leaves a broad swath of m_V and ϵ that are allowed by all collider experiments and cosmological bounds, and are capable of explaining the GC excess. The best prospects for discovering this model at the LHC would be through the exotic decay of the SM Higgs to the new vector boson, either in association with a Z boson, $h \rightarrow ZZ_D$, or in pairs, $h \rightarrow Z_D Z_D$, depending on the structure of the dark symmetry-breaking sector [53].

IV. CASCADE ANNIHILATION TO SCALAR MEDIATORS

In this section we consider simple reference models for DM annihilating to pairs of states which couple to the SM through the Higgs portal, i.e., have couplings to SM states proportional to their Yukawa couplings (at leading order). The simplest such model that allows for a present-day thermal cross-section of the correct order of magnitude is scalar DM annihilating to pairs of scalars. Fermionic DM annihilating to pairs of scalars, through DM-scalar annihilations alone, does not have any s -wave thermal cross-section, and is therefore not a compelling explanation for the observed GC excess.

We consider a simple Higgs portal scenario [54, 55]. We take the DM ϕ to be a complex scalar and let it carry a global $U(1)$ quantum number guaranteeing its stability (taking ϕ real and stabilized by a Z_2 parity would not materially affect our conclusions). We consider the interactions between ϕ , s , and h to be given by

$$V(\phi, s, H) = V(|\phi|^2) + V(|H|^2) + \frac{\lambda_4}{2} |\phi|^2 s^2 + \frac{\epsilon}{2} s^2 |H|^2 + \left(-\frac{\mu_s^2}{2} s^2 + \frac{\lambda_s}{4!} s^4 \right). \quad (12)$$

Suppose that the VEV $\langle s \rangle$ spontaneously breaks the Z_2 parity $s \rightarrow -s$ of the potential. After EWSB and Z_2 breaking, the mixing angle between s and h is then

$$\tan 2\theta \approx 2\theta = \frac{2\epsilon \langle s \rangle v}{m_h^2 - m_s^2}; \quad (13)$$

we take $\theta \ll 1$ and hence the physical masses $m_{s,h}^2$ are approximately equal to their unperturbed values. In general the interactions of Eq. (12) will induce the interaction $|\phi|^2 |H|^2$ at loop level; this will be negligible in comparison to the tree-level interactions in the regime of interest.

The independent parameters of this simple scalar reference model may be taken as m_ϕ , ϵ , $\langle s \rangle$, m_s , and λ_4 . Thus, compared to the dark vector model, we have one additional parameter: $y \equiv \langle s \rangle / m_s$, which we generically expect to be $\mathcal{O}(1)$. The thermal cross-section can be written

$$\langle \sigma v \rangle = \frac{1}{64\pi} \frac{\sqrt{1 - m_s^2/m_\phi^2}}{m_\phi^2} \lambda_4^2 \times \left(1 + \frac{3m_s^2}{4m_\phi^2 - m_s^2} - \frac{2\lambda_4 \langle s \rangle^2}{2m_\phi^2 - m_s^2} \right)^2 + \mathcal{O}(v^2). \quad (14)$$

Note that the dependence on y enters only in the last term in parentheses, multiplying λ_4 . Since we will find that $\lambda_4 \sim 10^{-2}$ to achieve the needed relic abundance, this renders the thermal relic abundance insensitive to y . In Fig. 7 (left) we show the value of λ_4 needed to yield the correct thermal relic abundance, as obtained using

the approximate analytic s -wave solution to the Boltzmann equation. Exact solution of the Boltzmann equation predicts present-day thermal cross-sections again in the range

$$\langle \sigma v \rangle|_{\text{today}} = (4.3 - 4.5) \times 10^{-26} \text{ cm}^3/\text{s}. \quad (15)$$

The leading contribution to direct detection is single s exchange, giving the per-nucleon cross-section

$$\sigma_{\phi N} = \frac{\mu^2}{4\pi m_\phi^2} f_N^2 \lambda_4^2 \epsilon^2 \left(\frac{\langle s \rangle^4}{m_s^4} \right) \left(\frac{m_N}{m_h^2 - m_s^2} \right)^2, \quad (16)$$

where $m_N \approx 0.94$ GeV is the nucleon mass. Again, we drop the subleading contribution from h exchange, as it is higher order in m_s^2/m_h^2 , and thus small in the region of most interest for the Fermi excess. Note the DM-nucleon scattering is proportional to y^4 ; thus the y dependence allows additional freedom to enhance or suppress the direct detection cross-section relative to signals from the GC or from the LHC. Fixing $y = 1$, we take the effective Higgs coupling to nucleons as $f_p = f_n = 0.345$ [56]³, and show the resulting constraints on the Higgs mixing ϵ in Fig. 7 (right). Constraints from direct detection are relatively weak, requiring $\epsilon \lesssim 0.4$ in the best-fit regions of parameter space.

More stringent constraints come from LHC limits on the total non-SM branching fraction of the Higgs, which limit $\text{Br}(h \rightarrow \text{BSM}) \lesssim 0.2$ if SM production is assumed [58–60]. In the mass ranges of interest for the GC excess, the scalar mass satisfies $m_s < m_h/2$. Thus the scalar potential of Eq. (12) yields a partial width for $h \rightarrow ss$,

$$\Gamma(h \rightarrow ss) = \frac{\epsilon^2 v^2}{32\pi m_h} \left(\frac{m_h^2 + 2m_s^2}{m_h^2 - m_s^2} \right) \sqrt{1 - \frac{4m_s^2}{m_h^2}}. \quad (17)$$

Requiring $\text{Br}(h \rightarrow ss) < 0.2$ restricts $\epsilon \lesssim 1.5 \times 10^{-2}$; future measurements of the Higgs sector with 5-10% precision [61] can be sensitive to $\epsilon \gtrsim 0.7 \times 10^{-3}$, as we show in Fig. 8. Values of $\epsilon \sim 10^{-3}$ correspond to $\theta \sim 10^{-4}$. Such values of θ still allow s to decay well before BBN in the mass ranges under consideration. As in the dark vector case, for $m_s \lesssim 10$ GeV there are additional limits from invisible quarkonium decay, but these are typically less constraining than the inclusive Higgs decay limit, giving limits of $\epsilon \lesssim 10^{-2}$ [62].

The small Yukawa couplings of the light SM fermions imply in general that for $\epsilon \lesssim 10^{-3}$, kinetic decoupling occurs at temperatures of the same order as the freeze-out temperature. Thus a full numerical solution of the Boltzmann equation would be required to precisely determine the relic abundance for a given λ_4 and ϵ . As kinetic decoupling again occurs prior to the chiral phase transition,

³ See Ref. [57] for an alternate approach to Higgs-nucleon couplings.

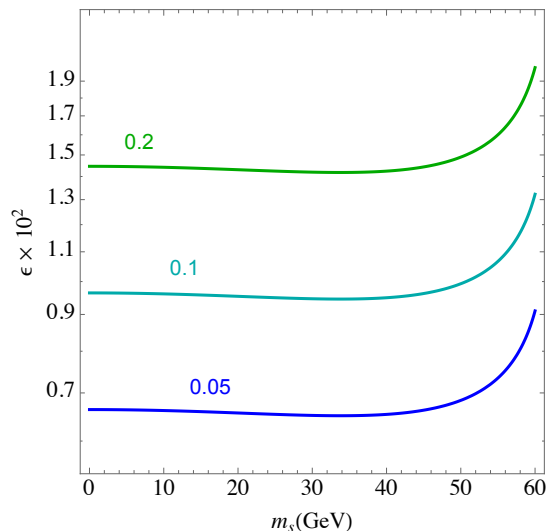


FIG. 8. Limits on the scalar-Higgs mixing parameter ϵ from Higgs properties at the LHC, as a function of mediator mass m_s . The three contours denote $\text{Br}(h \rightarrow ss) = 0.2, 0.1$, and 0.05 , as indicated.

the net impact on the deduced dark matter properties is small relative to the astrophysical uncertainties, and the approximate treatment presented here is sufficient to assess the relations between indirect, direct, and collider signals expected in this model.

For ϵ values consistent with $\text{Br}(h \rightarrow \text{BSM}) \lesssim 0.2$, s will be difficult to see at colliders. Direct observation of the exotic Higgs decays $h \rightarrow ss$, with s decaying according to the SM Yukawa couplings, will be challenging at the LHC; see [53] for a recent survey and review. The best prospects exist in the region $m_s < 2m_b$, where the enhanced $\text{Br}(s \rightarrow \tau\tau)$ may allow a detection for $\text{Br}(h \rightarrow ss) \gtrsim 5\%$; for $m_s > 2m_b$, sensitivity to $\text{Br}(h \rightarrow ss) \gtrsim 20\%$ is a reasonable target [53].

V. CASCADE ANNIHILATIONS TO GLUOPHILIC MEDIATORS

Let us re-examine the scalar DM model of Sect. IV in the case that $\langle s \rangle = 0$. To allow s to decay, we add to the spectrum a pair of heavy vector-like fermions ψ in the SM representation $(3, 1)_Y + \text{h.c.}$ which are coupled to the DM as follows:

$$\mathcal{L} \supset \frac{\lambda_4}{2} |\phi|^2 s^2 + \lambda_\psi s \psi \bar{\psi} - M \psi \bar{\psi}. \quad (18)$$

Integrating out these heavy exotic fermions leads to

$$\mathcal{L}_{\text{eff}} \supset \frac{\lambda_4}{2} |\phi|^2 s^2 + \frac{1}{\Lambda} s G_{\mu\nu}^a G^{a\mu\nu}. \quad (19)$$

The mass scale Λ can be identified with [63]:

$$\Lambda^{-1} = \frac{\alpha_S b_i \lambda_\psi}{8\pi M}. \quad (20)$$

where b_i is the β -function contribution due to ψ , e.g. $2/3$ for an SU(3) triplet. This scenario allows for cascade annihilations of the form $\phi\phi^\dagger \rightarrow ss$, and subsequently $s \rightarrow gg$. The resulting gamma-ray spectrum for this case is studied in Fig. 4 (right). The decay rate of the scalar state to gluons is

$$\Gamma_s = \frac{8 m_s^3}{4\pi \Lambda^2}. \quad (21)$$

Decays before BBN occur provided the coloured fermions have mass $M/\lambda_\psi \lesssim 10^{11}$ GeV. This coupling via exotic heavy fermions is analogous to KSVZ-type axion models [64, 65].

For $Y \neq 0$ the heavy fermion loop also induces the operator $s F_{\mu\nu} F^{\mu\nu}$ and thus also the decay $s \rightarrow \gamma\gamma$. This decay directly to photons would result in a gamma-ray line for s at rest in the galactic frame. In the case of interest for us, where $x = m_s/m_\phi \sim 0.5$, the boost of the s particles relative to the galactic frame widens the line into a box [66]:

$$\frac{1}{N_\gamma} \frac{dN_\gamma}{dE_\gamma} = \frac{1}{m_\phi \sqrt{1-x^2}} \Theta \left(E_\gamma - \frac{m_\phi}{2} (1 - \sqrt{1-x^2}) \right) \times \Theta \left(\frac{m_\phi}{2} (1 + \sqrt{1-x^2}) - E_\gamma \right). \quad (22)$$

The intensity of the gamma-ray box relative to the gluon-induced continuum contribution will be suppressed by the factor $(\alpha_{\text{em}}/\alpha_s)^2$, and is not currently observable for the parameters of interest [66]. On the other hand, the box extends to significantly higher photon energies E_γ and has a kinematic feature at the upper endpoint, and thus presents an interesting target for future experiments.

Similar to the previous cases, in Fig. 9 we show the value of λ_4 required to obtain the observed relic density. These results apply also to DM annihilations to pairs of pseudo-scalars, $\phi\phi \rightarrow aa$. For definiteness, we take the dark sector and the SM to be reheated to the same temperature $T_{\text{reheat}} > m_{\text{top}}$, but kinetically decoupled thereafter. As DM freeze-out occurs prior to the chiral phase transition in our best-fit regions ($m_{\text{DM}} \sim 40$ GeV), we approximate $T_{\text{DM}} = 0.83 T_{\text{SM}}$.

The leading direct detection cross-section is spin-independent and highly suppressed. Parameterizing the effective s -nucleon coupling as [67]⁴

$$g_{sNN} \simeq \frac{\langle N | GG | N \rangle}{\Lambda} \simeq -\frac{4\pi}{\alpha_s \Lambda} \times 180 \text{ MeV}, \quad (23)$$

⁴ The accuracy of the SU(3) chiral perturbation theory used to extract the gluonic matrix elements $\langle N | GG | N \rangle$ and $\langle N | G\tilde{G} | N \rangle$ has been questioned, and an alternate approach has recently been proposed for the scalar matrix element $\langle |m_f f \bar{f}| \rangle$ in Ref. [57]; however, as our aim here is to establish a parametric estimate, the precision is more than sufficient for our purposes.

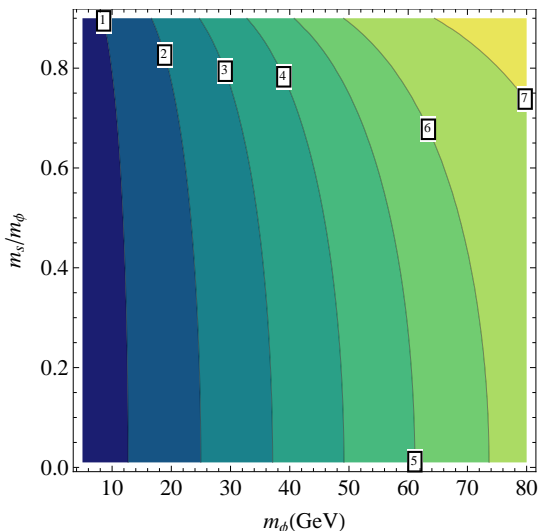


FIG. 9. The quartic coupling λ_4 needed to obtain $\Omega h^2 = 0.11$ for complex scalar DM ϕ annihilating to pairs of dark scalars s in the model of Sect. (V), as a function of m_ϕ and $m_s = xm_\phi$ (using the approximated s -wave solution to the Boltzmann equation). Contours show the required λ_4 in units of 10^{-2} .

direct detection proceeds at one-loop, with cross-section parametrically given by

$$\sigma_{\phi N} \sim \frac{1}{16\pi} \frac{1}{(m_\phi + m_N)^2} \frac{\lambda_4^2 g_{sNN}^4}{16\pi^2} \left(\frac{m_N}{m_s}\right)^4. \quad (24)$$

Clearly, for $M/\lambda_\psi \gg \text{TeV}$, there is no hope of a direct detection signal.

Similar results hold for pseudo-scalars a , although Λ is a factor of 3 larger. In this case, we estimate the effective a -nucleon coupling as [67]

$$g_{aNN} \simeq \frac{\langle N|G\tilde{G}|N\rangle}{\Lambda} \simeq -\frac{8\pi}{\alpha_s \Lambda} \times \begin{cases} -380 \text{ MeV} & p \\ 10 \text{ MeV} & n \end{cases} \quad (25)$$

The leading direct detection cross-section is spin-independent and highly suppressed, with similar parametric dependence to the scalar case.

VI. CONCLUDING REMARKS

If its origin from DM is confirmed, the GC gamma-ray excess will not only present the long-awaited detection of DM, but also provide evidence of a dark sector governing its interactions. The DM mass and thermal cross-section indicated by the excess is highly suggestive of a particle of mass $m_{\text{DM}} \sim \text{tens of GeV}$, freezing out via thermal annihilations mediated by a BSM particle, with a substantial component of the annihilation proceeding through the s -wave. For DM with this mass and this magnitude of coupling, the big challenge for models of DM is to reconcile the signal from the GC with the lack of any signal at direct detection experiments, especially LUX.

The deduced need for a BSM mediator naturally presents an elegant solution to this puzzle. When $m_{\text{med}} < m_{\text{DM}}$, the mediator itself is available as a final state for DM annihilations. A small coupling of the mediator to the SM subsequently allows the mediator to decay to SM particles with a cosmologically short lifetime. Thus in this scenario the coupling of the dark sector to SM particles in general and to nucleons in particular is no longer tied to the thermal relic density of DM. This cascade annihilation scenario opens up the scope of possible masses and quantum numbers for both DM and the mediator.

The photon spectra arising from cascade annihilations will be determined by the masses of the DM and mediator, together with the details of how the mediator decays. We have studied three well-motivated minimal scenarios for mediator decay: vector mediators decaying to the SM via hypercharge mixing; scalar mediators decaying to the SM through Higgs mixing; and (pseudo)-scalar mediators decaying to the SM via loops of heavy fermions. For all scenarios we establish the combinations of masses that lead to the best description of the gamma-ray spectrum, as determined in [10].

We construct simple reference models for all of these scenarios and demonstrate that they are capable of explaining the GC excess whilst naturally eluding direct detection as well as collider limits. Our best-fit scenarios are compared to the observations in Fig. 5. There is a large and natural range of parameter space in all of these models capable of explaining the excess. This ease in evading current experiments has the unfortunate consequence that signals of these models at direct detection and at colliders are naturally small, and may be difficult to observe at the LHC. Exotic decays of quarkonia and of the SM Higgs boson offer the best prospects for terrestrial experiments. Astrophysical signals offer a window onto the complementary regime where the mediator has small couplings to the SM, via perturbations of BBN or the CMB via late-decaying particles.

We have focused our attention on minimal models, with one DM particle and one mediator species active in the process of thermal freeze-out. Less minimal choices of mediator-SM couplings may also be constructed. For instance, hidden vectors may be constructed that couple to the SM through leptophobic [68–70] or leptophilic [71] portals. In such cases the DM thermal freeze-out will generically proceed as computed in Sect. IV, but the constraints on the mediator couplings to the SM, as well as limits on the additional matter species that appear in such models, will impose different restrictions on the allowed parameter space. Further, a much broader range of possible DM quantum numbers and interactions opens up if the mediator sector is allowed to be non-minimal, enabling such possibilities as mixed annihilations $XX \rightarrow \phi_1\phi_2$ [72], longer cascades [73], or showering in a hidden sector. There are many opportunities for extending DM model building in these directions.

ACKNOWLEDGEMENTS

We are grateful to Dan Hooper, Robert Lasenby, Tim Linden, Torbjörn Sjöstrand, and Tracy Slatyer for useful discussions. Note: Preprints [74–76], which appeared in the process of finalising this work, consider complementary aspects of DM cascade annihilations.

-
- [1] L. Goodenough and D. Hooper, [0910.2998].
- [2] D. Hooper and L. Goodenough, Phys. Lett. B **697**, 412 (2011) [1010.2752].
- [3] D. Hooper and T. Linden, Phys. Rev. D **84**, 123005 (2011) [1110.0006].
- [4] K. N. Abazajian and M. Kaplinghat, Phys. Rev. D **86**, 083511 (2012) [1207.6047].
- [5] D. Hooper, C. Kelso and F. S. Queiroz, Astropart. Phys. **46** (2013) 55 [1209.3015].
- [6] D. Hooper and T. R. Slatyer, Phys. Dark Univ. **2**, 118 (2013) [1302.6589].
- [7] C. Gordon and O. Macias, Phys. Rev. D **88**, 083521 (2013) [1306.5725].
- [8] W. -C. Huang, A. Urbano and W. Xue, [1307.6862].
- [9] K. N. Abazajian, N. Canac, S. Horiuchi and M. Kaplinghat, [1402.4090].
- [10] T. Daylan, D. P. Finkbeiner, D. Hooper, T. Linden, S. K. N. Portillo, N. L. Rodd and T. R. Slatyer, [1402.6703].
- [11] K. N. Abazajian, JCAP **1103**, 010 (2011) [1011.4275].
- [12] Q. Yuan and B. Zhang, [1404.2318].
- [13] D. Hooper, I. Cholis, T. Linden, J. Siegal-Gaskins and T. Slatyer, Phys. Rev. D **88**, 083009 (2013) [1305.0830].
- [14] T. Linden, E. Lovegrove and S. Profumo, Astrophys. J. **753** (2012) 41 [1203.3539].
- [15] O. Macias and C. Gordon, Phys. Rev. D **89** (2014) 063515 [1312.6671].
- [16] P. Agrawal, B. Batell, D. Hooper and T. Lin, [1404.1373].
- [17] A. Alves, S. Profumo, F. S. Queiroz and W. Shepherd, [1403.5027].
- [18] A. Berlin, D. Hooper and S. D. McDermott, [1404.0022].
- [19] C. Boehm, M. J. Dolan, C. McCabe, M. Spannowsky and C. J. Wallace, [1401.6458].
- [20] S. Ipek, D. McKeen and A. E. Nelson, [1404.3716].
- [21] E. Izaguirre, G. Krnjaic and B. Shuve, [1404.2018].
- [22] G. Marshall and R. Primulando, JHEP **1105** (2011) 026 [1102.0492].
- [23] M. S. Boucenna and S. Profumo, Phys. Rev. D **84** (2011) 055011 [1106.3368].
- [24] D. Hooper, N. Weiner and W. Xue, Phys. Rev. D **86** (2012) 056009 [1206.2929].
- [25] K. Hagiwara, S. Mukhopadhyay and J. Nakamura, Phys. Rev. D **89** (2014) 015023 [1308.6738].
- [26] K. C. Y. Ng, R. Laha, S. Campbell, S. Horiuchi, B. Dasgupta, K. Murase and J. F. Beacom, Phys. Rev. D **89** (2014) 083001 [1310.1915].
- [27] N. Okada and O. Seto, Phys. Rev. D **89**, 043525 (2014) [1310.5991].
- [28] B. Kyae and J. -C. Park, Phys. Lett. B **732** (2014) 373 [1310.2284].
- [29] K. P. Modak, D. Majumdar and S. Rakshit, [1312.7488].
- [30] E. Hardy, R. Lasenby and J. Unwin, [1402.4500].
- [31] K. Kong and J. -C. Park, [1404.3741].
- [32] M. Pospelov, A. Ritz and M. B. Voloshin, Phys. Lett. B **662**, 53 (2008) [0711.4866].
- [33] M. Cirelli, *et al.*, JCAP **1103** (2011) 051 [Erratum-ibid. **1210** (2012) E01] [1012.4515].
- [34] J. F. Navarro, C. S. Frenk and S. D. M. White, Astrophys. J. **462** (1996) 563 [astro-ph/9508025].
- [35] J. F. Navarro, C. S. Frenk and S. D. M. White, Astrophys. J. **490** (1997) 493 [astro-ph/9611107].
- [36] F. Iocco, M. Pato, G. Bertone and P. Jetzer, JCAP **1111** (2011) 029 [1107.5810].
- [37] T. Sjostrand, S. Mrenna and P. Z. Skands, Comput. Phys. Commun. **178**, 852 (2008) [0710.3820].
- [38] M. Cirelli, P. D. Serpico and G. Zaharijas, JCAP **1311** (2013) 035 [1307.7152].
- [39] B. Holdom, Phys. Lett. B **166**, 196 (1986).
- [40] P. Galison and A. Manohar, Phys. Lett. B **136**, 279 (1984).
- [41] S. Gopalakrishna, S. Jung and J. D. Wells, Phys. Rev. D **78** (2008) 055002 [0801.3456].
- [42] A. Djouadi, J. Kalinowski and M. Spira, Comput. Phys. Commun. **108**, 56 (1998) [hep-ph/9704448].
- [43] J. M. Butterworth, *et al.*, [1003.1643].
- [44] N. Arkani-Hamed, D. P. Finkbeiner, T. R. Slatyer and N. Weiner, Phys. Rev. D **79** (2009) 015014 [0810.0713].
- [45] M. R. Buckley and P. J. Fox, Phys. Rev. D **81** (2010) 083522 [0911.3898].
- [46] D. N. Spergel and P. J. Steinhardt, Phys. Rev. Lett. **84** (2000) 3760 [astro-ph/9909386].
- [47] J. L. Feng, M. Kaplinghat and H. -B. Yu, Phys. Rev. Lett. **104** (2010) 151301 [0911.0422].
- [48] D. S. Akerib *et al.* [LUX Collaboration], [1310.8214].
- [49] M. Kaplinghat, S. Tulin and H. -B. Yu, Phys. Rev. D **89**, 035009 (2014) [1310.7945].
- [50] R. Essig, *et al.*, [1311.0029].
- [51] A. Hook, E. Izaguirre and J. G. Wacker, Adv. High Energy Phys. **2011**, 859762 (2011) [1006.0973].
- [52] B. Aubert *et al.* [BaBar Collaboration], Phys. Rev. Lett. **103** (2009) 251801 [0908.2840].
- [53] D. Curtin, *et al.*, [1312.4992].
- [54] B. Patt and F. Wilczek, [hep-ph/0605188].
- [55] J. March-Russell, S. M. West, D. Cumberbatch and D. Hooper, JHEP **0807** (2008) 058, [0801.3440].
- [56] J. M. Cline, K. Kainulainen, P. Scott and C. Weniger, Phys. Rev. D **88**, 055025 (2013) [1306.4710].
- [57] A. Crivellin, M. Hoferichter and M. Procura, Phys. Rev. D **89** (2014) 054021 [1312.4951].
- [58] G. Belanger, B. Dumont, U. Ellwanger, J. F. Gunion and S. Kraml, Phys. Lett. B **723**, 340 (2013) [1302.5694].
- [59] P. P. Giardino, K. Kannike, I. Masina, M. Raidal and A. Strumia, JHEP **1405**, 046 (2014) [1303.3570].
- [60] J. Ellis and T. You, JHEP **1306**, 103 (2013) [1303.3879].

- [61] M. E. Peskin, [1312.4974].
- [62] R. Essig, J. Mardon, M. Papucci, T. Volansky and Y. - M. Zhong, JHEP **1311** (2013) 167 [1309.5084].
- [63] S. Chang, P. J. Fox and N. Weiner, JHEP **0608**, 068 (2006) [hep-ph/0511250].
- [64] J. E. Kim, Phys. Rev. Lett. **43** (1979) 103.
- [65] M. A. Shifman, A. I. Vainshtein and V. I. Zakharov, Nucl. Phys. B **166** (1980) 493.
- [66] A. Ibarra, S. Lopez Gehler and M. Pato, JCAP **1207**, 043 (2012) [1205.0007].
- [67] H. -Y. Cheng and C. -W. Chiang, JHEP **1207**, 009 (2012) [1202.1292].
- [68] K. S. Babu, C. F. Kolda and J. March-Russell, Phys. Rev. D **54** (1996) 4635 [hep-ph/9603212].
- [69] B. A. Dobrescu and C. Frugiuele, [1404.3947].
- [70] S. Tulin, [1404.4370].
- [71] P. J. Fox and E. Poppitz, Phys. Rev. D **79** (2009) 083528 [0811.0399].
- [72] Y. Nomura and J. Thaler, Phys. Rev. D **79**, 075008 (2009) [0810.5397].
- [73] J. Mardon, Y. Nomura, D. Stolarski and J. Thaler, JCAP **0905**, 016 (2009) [0901.2926].
- [74] C. Boehm, M. J. Dolan and C. McCabe, [1404.4977].
- [75] P. Ko, W. -I. Park and Y. Tang, [1404.5257].
- [76] M. Abdullah, A. DiFranzo, A. Rajaraman, T. M. P. Tait, P. Tanedo and A. M. Wijangco, [1404.6528].